THE CONTRIBUTION OF THE RIIHIMAA CLASSIFICATION TO THE STUDY OF JOVIAN MILLISECOND RADIO BURSTS

M. Y. Boudjada*, H. O. Rucker*, P. H. M. Galopeau†,
P. Kleewein‡, and V. Mostetschnig*

Abstract

A morphology classification was introduced by Riihimaa [1991] showing sketches of various types of individual S-bursts based on observations recorded between 1970 and 1989 at Oulu University (Finland). With this classification it was possible to distinguish one S-burst from another by its form and its spectral characteristics in time and frequency.

Using this classification two aspects can be discussed. The first one concerns the existence of correlation between the S-burst pattern as an ensemble containing S-bursts and the inherent individual S-bursts. When taking into account the spectra of different S-bursts it appears that the drift of the S-burst pattern is a function of the structure, like **type b** and **type f**. The second aspect concerns the measurement of the S-burst drift rates which can be deduced from the observations. It appears from Riihimaa's classification that some structures, as **type f,** display both positive and negative drift rates. In this case it is not possible to explain the drift rate using only the classical model based on the hypothesis of an adiabatic motion of trapped electrons.

1 Introduction

Nonthermal radio emissions from Jupiter at decametric wavelengths (hereafter DAM) have been discovered by Burke and Franklin in 1955 [Burke and Franklin, 1955]. Long-term ground observations revealed that the occurrence probability of the radiation is a function of the Jovian Central Meridian Longitude (CML) and the orbital position of the innermost Galilean satellite, Io, relative to the observer [Bigg, 1964]. In the CML-Io

*Space Research Institute, A-8010 Graz, AUSTRIA
†Centre d'Étude des Environnements Terrestre et Planétaires, Centre National de la Recherche Scientifique, F-78140 Vélizy, FRANCE
‡Laboratoire d'Electronique, Observatoire de Meudon, F-92195 Meudon, FRANCE

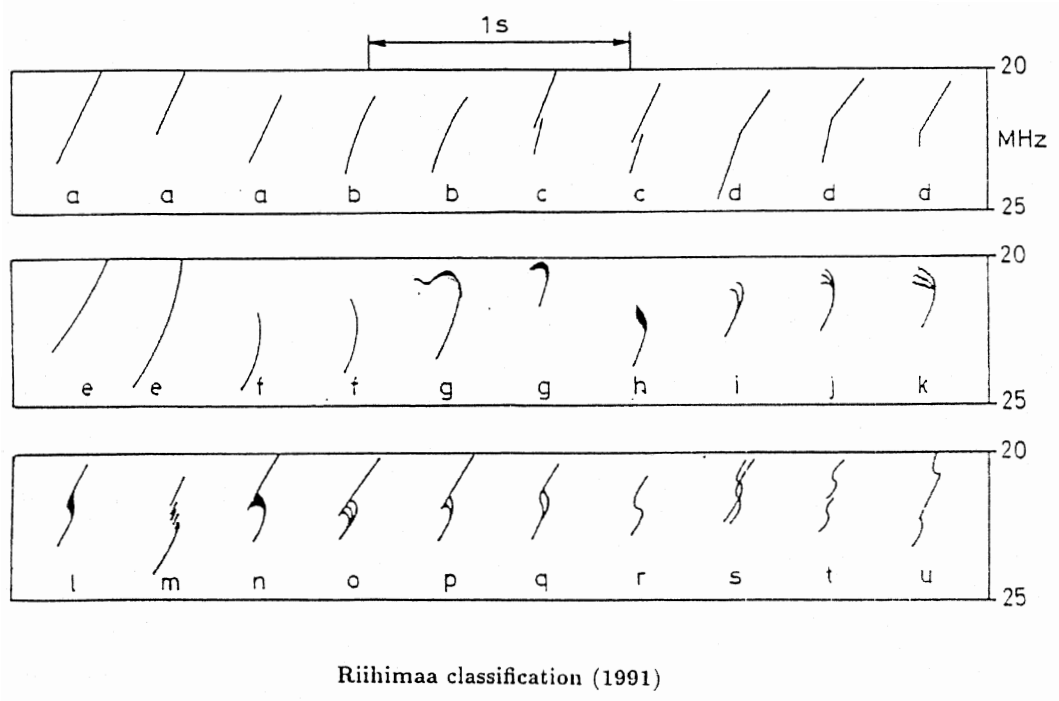

Figure 1: Schematics of individual S-burst spectra, as reported by Riihimaa [1991], with their correct frequency ranges, frequency-time aspect ratios and spectral locations.

phase plane three principal regions are called sources (A, B, C) and each one consists of Io-related and Io-unrelated components [Carr et al., 1983].

Frequency-time dynamic spectra of DAM emission are organized in two different types of storms according to the time scale. The L-burst emission appears as a smooth emission of several minutes duration and an instantaneous frequency range of a few MHz. The S-burst emissions have single-frequency durations of 1 to 200 ms, a narrow instantaneous bandwidth and a rapid frequency drift in time ranging from -5 to -45 MHz/s. The S-bursts account for a relatively small fraction of the DAM emission ($\simeq$ 10%). Their narrower occurrence in CML and Io phase probably indicates that the S-burst emission is more directive than the L-burst emission. The spectral properties of S-bursts have been studied in a number of papers and many examples of their fine structure with very high time and frequency resolution can be found in Ellis [1979], Flagg et al. [1991], Riihimaa [1992], and Ryabov et al. [this volume]. The first structure classification was presented by Riihimaa [1991] who gave a schematic representation of the most common variants of individual S-bursts, in the frequency range from 20 to 25 MHz. The author reported on S-bursts as they appear in dynamic spectra (see Figure 1) recorded at Kiiminki site (Finland) between 1974 and 1989.

Several studies have been devoted to the analysis of the S-burst drift rates with a view toward an understanding of the S-burst emission process. Ellis [1974] established a model in which trapped electrons, accelerated at Io, gyrate around magnetic field lines and bounce between their mirror points emitting radiation at the local gyrofrequency. The drift rate (DR) was measured dominantly negative [Ellis, 1975; Krausche et al., 1976; Desch et al., 1978; Riihimaa, 1979; Leblanc et al., 1980b; Boudjada et al., 1995; Zarka

et al., 1996]. According to the Ellis model the negative DR is interpreted as an effect of radiation observed after the reflection of the electrons from their mirror points.

In the following we report on two analyses based on Riihimaa's classification. In Section 2, we analyse the physical parameters (frequency range, constant frequency duration and drift rate) of the fine structure (individual burst) and their change from one pattern of S-bursts to another. Simulating and calculating the drift rate of one structure (**type f**), we compare it in Section 3 to the classical model used to explain the S-burst drift rates. In the final part we discuss our results and future investigations.

2 Individual S-bursts organization inside an S-burst pattern

This analysis of Jovian millisecond radio bursts is based on observations made at the radio station Graz-Lustbühel on January 4^{th}, 1993. This event has been recorded simultaneously at two others stations, Nançay in France and Kharkov in Ukraine. The three radiotelescopes are separated in longitude by approximately 15°, but located at nearly the same northern latitude ($\simeq 48°$). This network allows us to use different receivers with complementary characteristics (multichannel receiver at Graz and Kharkov, spectro-analyser and spectro-polarimeter at Nançay). Observation was made during periods of S-burst activity within an Io-B storm. The event occurred on Jan. 4^{th}, 1993, between 0345 and 0558 UT. In this particular interval the Jovian central meridian longitude ranged from 104° to 185° and the Io phase changed from 81° to 100°.

2.1 Observations of the event of January 4, 1993

The main S-burst emission begins at 0420 UT, and twenty minutes later the first L-burst becomes visible. During the subsequent ten minutes both structures L- and S-bursts coexist and at 0500 UT the S-burst emission starts disappearing, whereas the L-burst emission continues till 0550 UT. Figure 2 shows the observation coverage, in frequency and time, for each station and the used receivers. Apparently, Jupiter was continuously recorded over ten hours which covers one rotation period.

The first emissions observed by the Kharkov Observatory [Braude et al., 1978] were recorded at low frequencies, between 10 and 17 MHz, at 0100 UT. These radiations correspond to L-burst emissions. Nearly three hours later at Nançay station [Boischot et al., 1980b] the first S-burst pattern clearly appeared (see Figure 3). The S-storm activity becomes intense and more complex, at 0425 UT, in particular at frequencies between 16 and 24.5 MHz. Twenty minutes later, another type of structures, L-bursts, appeared at frequencies $f \geq 18$ MHz. At the same time the S-burst intensity decreases and starts being superposed by the L-bursts.

At Lustbühel Observatory (Rucker et al., 1992) the radiation is observed at 0428 UT when the Jovian emission becomes more intense. During six consecutive minutes, S-storm activity is recorded in the range of 23 to 25 MHz. The S-burst frequency range is found, on average, to be less than 300 kHz with a variable constant-frequency duration (CFD)

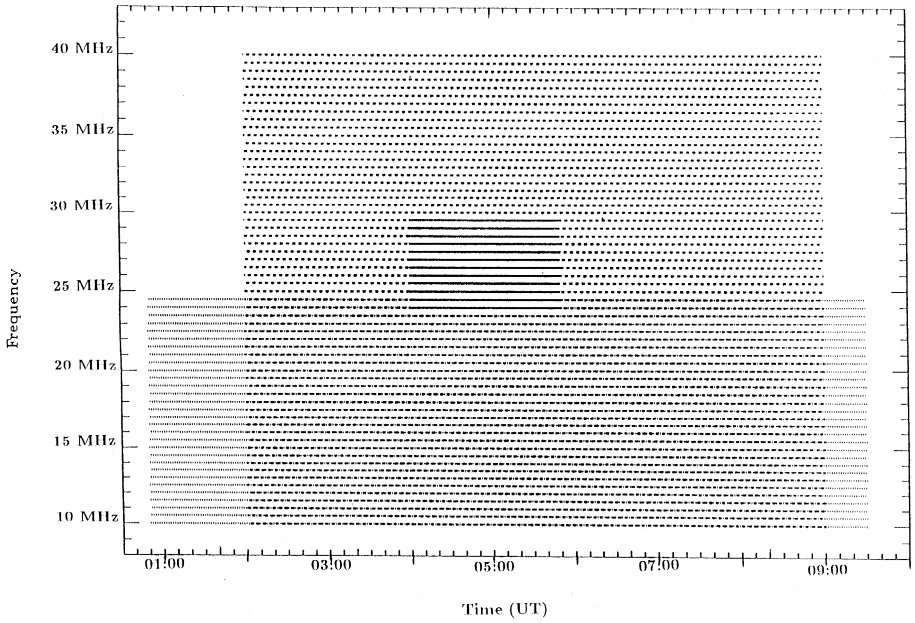

Figure 2: The coverage of the 4^{th} Jan. 1993 event by the three stations: Kharkov (Ukraine) with dotted lines, Graz (Austria) with solid lines and Nançay (France) with dashed lines in the figure. The total time of observation is 10 hours where almost half an hour corresponds to S-bursts emission (04:30 to 05:00 UT). The used receivers are: (a) for Nançay Observatory: spectrum analyser (receiver band frequency $\Delta f_b = 30$ MHz; frequency resolution $\Delta f_r = 30$ kHz; time resolution $\Delta t = 350$ ms), (b) for Graz Observatory: multichannel receiver ($\Delta f_b = 1$ MHz, $\Delta f_r = 20$ kHz, $\Delta t = 2$ ms), (c) for Kharkov Observatory: multichannel receiver ($\Delta f_b = 15$ MHz, $\Delta f_r = 250$ kHz, $\Delta t = 50$ ms).

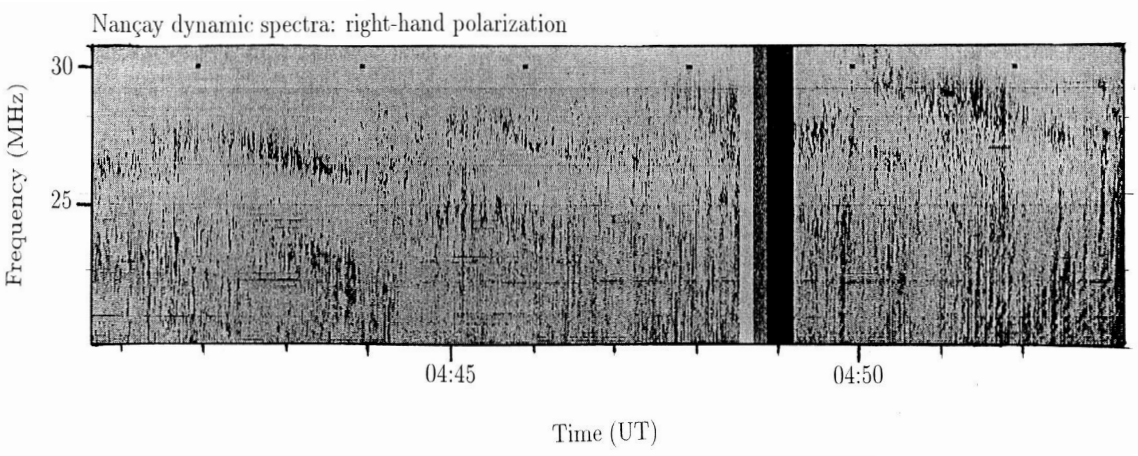

Figure 3: Nançay dynamic spectrum with distinguishable parts of S-burst patterns. Each pattern corresponds to an ensemble of dots assembling in the same area within the dynamic spectrum.

between 8 and 30 ms. We note the presence of individual S-bursts where two types could be distinguished. Bursts with structures like those reported by Riihimaa [1991] and others with irregular circular form thereafter have been called **puff**. The main difference with regard to the S-bursts in the Riihimaa classification is in the structure and in the

CFD which is about three times longer for the **puff** bursts. The occurrence of emission increases when the S-burst emission reaches frequencies higher than 25 MHz, as observed at 0435 UT. We find that the frequency range for the S-bursts is greater (600 kHz) than observed before. For **puff** bursts the only change can be seen in the intensity. Contrary to the precedent part, we observe quasi-periodic structures with curvatures due to decreasing, as **type b**, or increasing slopes, as **type f**. Sometimes the quasi-periodic bursts are superposed to a narrow band emission (Δf = 200 kHz) without drift. During this period we have an alteration, succession or superposition of the common variants of S-bursts as reported by Riihimaa [1991]. Table 1 gives observation parameters of the individual S-bursts; more details about the distribution and the frequency drift for the main structures are reported by Boudjada et al. [1995].

Table 1: Physical parameters of the individual S-bursts as observed at Graz: frequency range (FR), constant frequency duration (CFD) and drift rate (DR). Note that for the **types f** *and* **g** *positive and negative DR was observed.*

type	FR (kHz)	CFD (ms)	DR (MHz/s)
a	350	10	−33.8
b	475	10	−36.8
e	706	9	−29.8
f	560	10	−39.0
f	361	14	+62.5
g	540	17	−32.8
g	360	14	+40.6
Puff	208	32	–

2.2 Analysis of S-burst patterns

At Nançay Observatory the S-bursts appear as S-burst patterns. The large frequency band of the spectrum analyser (400 channels) makes visible more than 23 patterns of S-bursts. Because of the coarse resolution in time (350 ms), S-bursts can only be seen as points more intense than the other pixels within the dynamic spectrum (Figure 3). The drift rate of the global pattern envelope is mainly negative and in the order of −35 kHz/s with a frequency range of about 2.5 MHz. When the L-burst appears, the S-burst patterns seem to be pushed away toward higher frequencies, at the same time connected to L-burst patterns.

The distribution of the main individual S-bursts within each pattern showed that the patterns with negative drift have the same internal structures: **type a**, **type f** and the **puff**. **Type a** is found in that part of the pattern without any drift, the **type f** usually is found in the arc-curvature of the pattern, and the **puff** everywhere. The consecutive pattern seems to have the same internal structure (i.e. the same individual S-burst structures). When the pattern has a positive drift we find: **type a**, **type b** and

the **puff** with the same distribution as in the previous case, but the **type f** is replaced by **type b**. From this analysis it appears that the form of the S-burst pattern is due to the **types a, b** and **f**, whereas the **puff** gives the global shape.

3 Simulated drift rate of type f

The classical model invoked for the explanation of the negative DR was proposed by Ellis [1974]. This model relies on two fundamental parameters: the electron speed v and its initial pitch angle Φ_{E} at the magnetic equator. Fixing Φ_{E} and v, it is possible to derive the variation of the S-burst drift rate (df/dt) versus emission frequency f from the following expression:

$$\frac{df}{dt} = \pm\frac{3fv}{LR_{\mathrm{J}}} \cdot A(\theta) \cdot \sqrt{1 - \sin^2\Phi_{\mathrm{E}}\frac{(1+3\cos^2\theta)^{1/2}}{\sin^6\theta}}$$

where L is the magnetic shell parameter ($L \cong 6$ at Io), R_{J} the Jovian radius, and $A(\theta) = \cos\theta(3+5\cos^2\theta)/\sin^2\theta(1+3\cos^2\theta)^{3/2}$ is an expression depending on θ, the magnetic colatitude; df/dt is positive (negative) for electrons streaming inward to (outward from) their mirror point. Figure 4 shows the DR versus f, and we can distinguish two parts on the curve: a slow increase until a maximum, followed by a strong decrease until a high frequency cutoff where the drift rate should be virtually equal to zero. Almost all measurements of DR confirmed only the increase of drift rate versus frequency. Recently, Zarka et al. [1996] showed the decrease of DR with increasing frequency, as predicted by the Ellis model [1974].

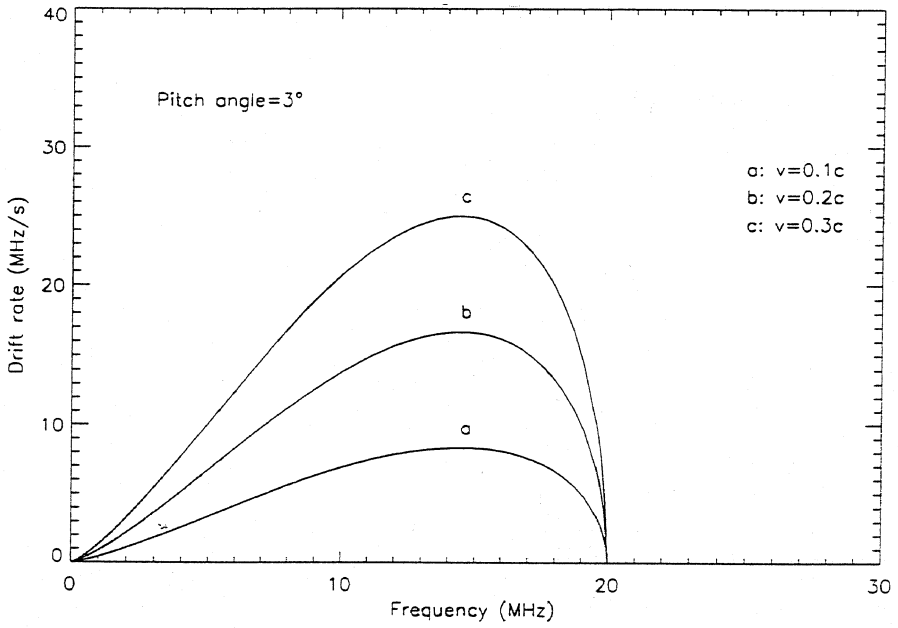

Figure 4: Example of curves showing the variation of the drift rate versus frequency deduced from the "trapped electron hypothesis" of the Ellis model for a fixed pitch angle and variable speed. It clearly appears that the increase in the speed enables higher drift rates.

We proceed to a simulation of three structures (Figure 5) as reported by Riihimaa [1991] in his classification. In Table 2, we list an example of the DR for a typical **type f** burst: It appears that the DR can be positive, negative and infinite. One can see that the DR for a typical S-burst structure, as **type f**, presents a decrease of DR for increasing frequencies, as predicted by the Ellis model in the second part of the drift versus frequency profile (Figure 4), but three questions emerge from Table 2:
a) What is the significance of the infinite value observed for the DR?
b) How can we explain the positive drift rate?
c) As shown in Boudjada et al. [1996], it is not possible to fit the DR values of one particular **type f** burst (Table 2) by only one Ellis model profile (Figure 4), determined by fixed values of Φ_E and v (Figure 6). How can this problem be solved?

These questions cannot be solved in the frame of the Ellis model. Our result is in some aspects in contradiction with the findings of Zarka et al. [1996]. They used observations collected by an acousto-optic spectrograph in a 26 MHz bandwidth, and high time and frequency resolutions, 10 msec and 13 kHz, respectively. They reported, in Figure 3 of their article, drift rates estimated over a band of 1 MHz, which could introduce an error on the DR measurement. From our simulated drift rates (Table 2) the error could be in the order of 100% when considering a band of 1 MHz. The drift rates change, e.g., from -57.4 MHz/s to -12.5 MHz/s within the frequency range from 22.8 and 23.8 MHz, respectively.

Table 2: Results of the simulated drift rate deduced from **type f** *structure. We note that both positive and negative drift rates could be calculated; an infinite value of DR appears when the drift rate changes sign.*

Freq. (MHz)	Drift (MHz/s)	Freq. (MHz)	Drift (MHz/s)
21.3	+12.20	22.6	∞
21.4	+12.55	22.7	−114.19
21.5	+13.06	22.8	−57.41
21.6	+13.78	22.9	−38.62
21.7	+14.75	23.0	−29.34
21.8	+16.06	23.1	−23.87
21.9	+17.83	23.2	−20.30
22.0	+20.30	23.3	−17.83
22.1	+23.87	23.4	−16.06
22.2	+29.34	23.5	−14.75
22.3	+38.62	23.6	−13.78
22.4	+57.41	23.7	−13.06
22.5	+114.19	23.8	−12.55
		23.9	−12.20
		24.0	−12.00
		24.1	−11.93

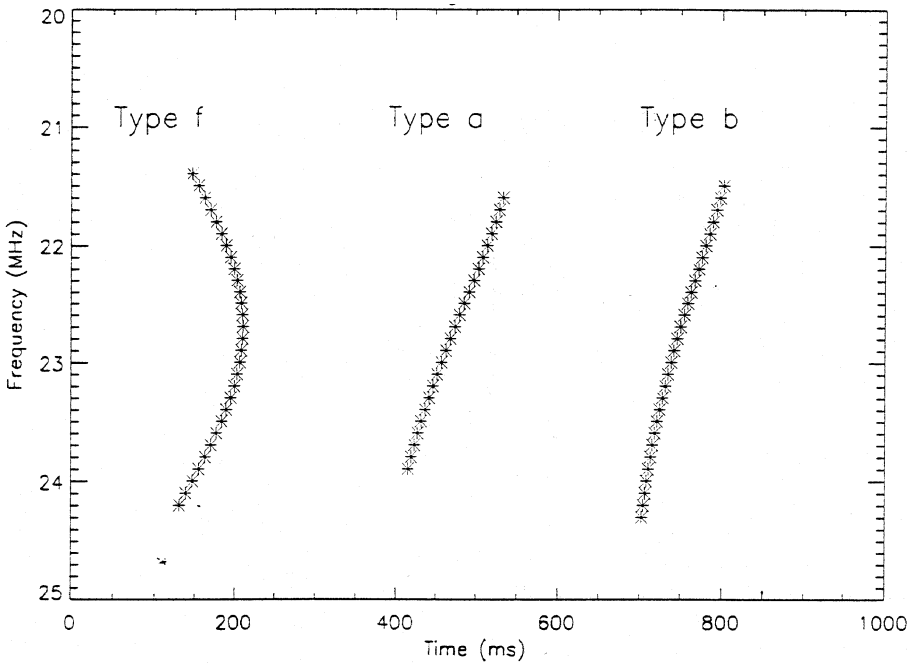

Figure 5: Simulation of three S-burst structures as reported by Riihimaa [1991]. From these structures one can see that **type a** *has an almost constant drift rate (DR) contrary to* **type b** *which presents a variable DR, usually negative, or the* **type f** *which displays both positive and negative DR.*

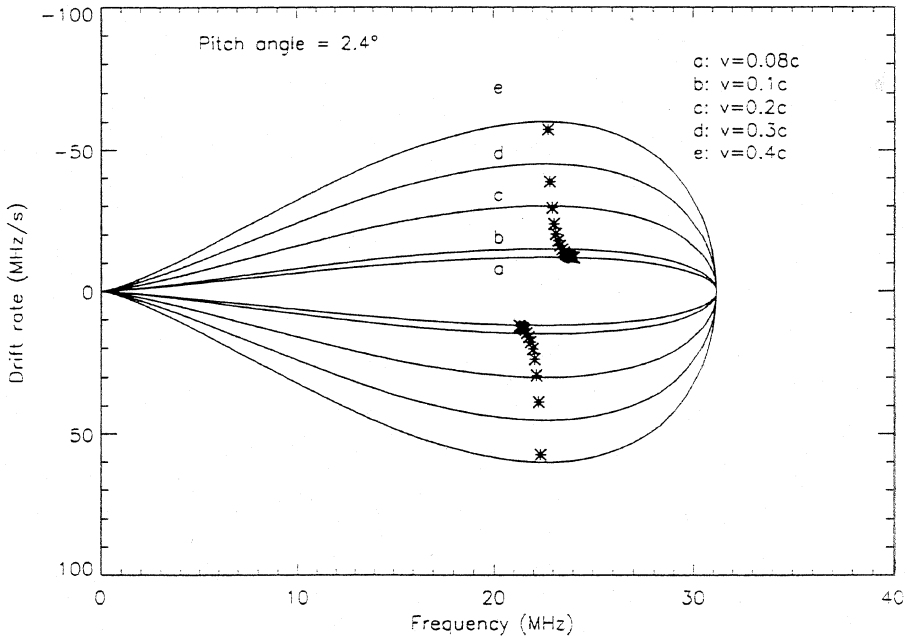

Figure 6: Theoretical curves from the Ellis model are compared to the simulated drift rate (presented as stars in the figure) enlisted in Table 1.

4 Discussion and Conclusion

We have used Riihimaa's classification to analyse two important aspects of the Jovian millisecond radio bursts: their phenomenology and their drift rate with regard to the classical model. For the first time an organisation of individual S-bursts inside an S-burst pattern is described. It appears from our analysis that in the drifting part of the pattern we have found the **type f** and **type b**, and the **type a** occurs mainly in the non-drifting part of the pattern.

By simulating and calculating the drift rate of one structure (**type f**) we have compared it to the Ellis model. The drift rates have been observed usually being negative and rarely being positive. The **type f** taken as an example is a typical S-burst with both positive and negative drift rates which has never been included and compared to the Ellis model. When we take in consideration the variable instantaneous drift rate of the same burst structure we show that it is not possible to fit the actual DR if both the pitch angle and the particle velocity are fixed, as found in previous studies. It is thus necessary to consider a distribution of velocities and pitch angles of the electrons, in order to fit a main part of the DR deduced from simulations. Obviously not only one single electron radiates but a packet of electrons (with their own individual Φ_{E} and v) following a bunch of magnetic field lines. This result is in concurrence with the recent investigation of Carr et al. [this volume] who showed that an individual S-burst is a combination of subsequent micro-structures.

We show by our analysis that it is possible to explain some of the S-burst phenomenology using Riihimaa's classification but some questions still remain open:
a) What is the origin of the gap between the S-burst patterns?
b) Why does one observe a correlation between the S- and the L-bursts [Riihimaa et Carr, 1981; Boudjada et al., 1995]?
c) Does exist a fundamental structure from where we could explain all the Riihimaa classification?
d) Which type of acceleration mechanism could explain the different types of structure as reported by Riihimaa?

All these questions need a continuation of Jovian millisecond radio bursts observations with more sensititive radiotelescopes [Ryabov et al., this volume] and possibly a new generation of radio receivers [Kleewein et al., this volume].